Journal of Engineering Sciences
Vol 12, Issue 7, July/2021
ISSN NO:0377-9254

MODELLING AND IMPLEMENTATION OF UPQC INTEGRATED PV MPPT SYSTEM FOR POWER QUALITY IMPROVEMENT

K. Keerthana[1], B.Ravi Chandra Rao[2]

[1]*Student of MTech, EEE, G.Narayanamma Institute of Technology and Science, India*

[2]*Assistant Professor, EEE, G.Narayanamma Institute of Technology and Science, India*

***Abstract*— PV integrated UPQC is a paper that comprises of a shunt and series-connected voltage compensator coupled back-to-back with a similar DC connection. The shunt filter controller serves two purposes: it extracts electricity from the PV array and it compensates for load current harmonics. Synchronous reference frame control is utilized to extract the load active current component. The series filter controller is used to correct for power quality issues such as grid voltage sag or voltage swells on the grid side. The compensator injects voltage in-phase or out-phase with the point of common coupling (PCC) voltage under sag and swell events. MATLAB with SIMULINK is used to simulate the steady-state performance**.

Keywords— **FLC, MPPT, Solar PV, Series filter controller, Shunt filter controller,**

1. INTRODUCTION

The prevalence of power electronic loads has risen as semiconductor technology has evolved. Computer power supplies, adjustable speed drives, switched mode power supplies, and other loads have high efficiency, yet they draw nonlinear currents. In distribution systems, these nonlinear currents produce voltage distortion at the point of common coupling. Due to the fluctuation of PV energy sources, high demand of such systems, particularly in weak distribution networks, causes voltage quality issues such as voltage sags and swells, resulting in grid instability [1], [2], [3], [4], [5]. These voltage quality issues also result in frequent erroneous tripping of power electronic systems, electronic system malfunctions and false triggering, and increased heating of capacitor banks, among other things [6], [7], [8]. A three-phase multi-functional solar energy conversion system has been suggested that adjusts for load-side power quality problems [9], [10].

A solar photovoltaic system with a dynamic voltage restorer has been suggested [11]. A unified power quality conditioner (UPQC), which contains both series and shunt compensators, can conduct load voltage control and maintain grid current sinusoidal at unity power factor at the same time, as opposed to shunt and series active power filters. When a PV array is combined with UPQC, it provides both clean energy generation and universal active. [12], [13], [14] have described the integration of a PV array with UPQC.

PVUPQC's control system relies heavily on reference signal generation. The time-domain and frequency-domain approaches for generating reference signals can be significantly classified [6]. Time domain methods are often employed in real-time implementation. Time domain methods include instantaneous reactive power theory (p-q theory) and synchronous reference frame theory (d-q), and symmetrical component theory (s-q theories) [15]. The primary disadvantage of using a synchronous reference frame theory-based technique is that the d-axis currents have a very low cutoff frequency. As a result, dynamic performance suffers. [16]. The d-axis current is filtered using a moving average filter (MAF) to get fundamental load active current. This provides optimum attenuation without decreasing the controller's bandwidth [17]. MAF has recently been used to improve the performance of DC-link controllers and grid synchronization utilizing phase locked loops (PLL). The design and performance study of a three-phase PV integrated UPQC are described in this work [18].

1. IMPLEMENTING A THREE PHASE SOLAR PV INTEGRATED UPQC SYSTEM:

The PVUPQC is made up of a shunt and a series filter controller that are both linked to a similar DC bus. Shunt filter controller adjusts for grid voltage sags, voltage swells while in voltage control mode. The solar PV array is directly connected to UPQC's DC-link. Figure 1 shows the PV-construction.

PV-UPQC design includes correct PV array sizing, DC-link capacitor sizing and voltage level sizing. The shunt filter controller is sized to accommodate the peak power output from the PV array.

a) VOLTAGE MAGNITUDE OF DC LINK: The size of the DC link voltage Vdc is determined by the depth of modulation employed, the system's per-phase voltage. The magnitude of the DC-link voltage should be more than double that of the three-phase system's peak per-phase voltage [6]. The equation is stated below,

m = modulation depth

v_{LL}= grid line voltage of 677.7v

$$V_{dc} = \frac{2\sqrt{2}v_{LL}}{\sqrt{3}m} \quad (1)$$

DC-bus voltage for a line voltage of 415 V is 677.7 V. The DC-bus voltage is set to 700 V (approximately), which is the same as the PV array's MPPT working voltage under standard temperature conditions (STC) circumstances.

b) DC-BUS CAPACITOR: The size of the DC-link capacitor is determined by the amount of power required as well as the DC-bus voltage level. [8], which is the energy balance equation for the DC-bus capacitor, and the equation is,

V_{dc} = average voltage of DC-bus,

V_{dc1}= lowest value of DC-bus voltage,

a = overloading factor,

V_{ph} = per-phase voltage,

t = minimum time required for achieving steady value after a disturbance,

I_{sh}= per-phase current of shunt filter controller,

k factor = energy variation during dynamics.

$$C_{dc} = \frac{3kaV_{ph}I_{sh}t}{0.5 \times (V_{dc}^2 - V_{dc1}^2)} \quad (2)$$

c) INTERFACING INDUCTOR FOR SHUNT FILTER CONTROLLER: The shunt filter controller's interface inductor rating is determined by the ripple current, switching frequency, and DC-link voltage. The interfacing inductor's expression is as follows:

m = depth of modulation,

a = per unit value of maximum overload,

f_{sh} = switching frequency,

$I_{cr,pp}$ = inductor ripple current which is considered as 20% of rms phase current of shunt filter controller.

$$L_f = \frac{\sqrt{3}mV_{dc}}{12\alpha f_{sh} I_{cr,pp}} = \frac{\sqrt{3} \times 1 \times 700}{12 \times 1.2 \times 10000 \times 6.9} \quad (3)$$

Here, m=1, a=1.2, f_{sh}=10kHz, V_{dc}=700V, we get 800μ H as value. The selected value is around 1mH.

d) SERIES INJECTION TRANSFORMER: The system has been designed to compensate for a sag or swell of 0.3 p u i.e., 71.88 V. The required voltage is 71.88 V which is injected into the series filter controller and the DC-link voltage is taken as 700V. To run with minimum harmonics, the modulation index is kept near to unity. Hence, the series transformer is employed with a turns-ratio,

$$K_{SE} = \frac{V_{vsc}}{V_{SE}} = 3.33 \approx 3 \quad (4)$$

The derived value for K_{SE} is 3.33 and the value selected is 3. The series injection transformer rating be given as,

$$S_{SE} = 3V_{SE} I_{SE\ sag} = 3 \times 72 \times 46 = 10kVA \quad (5)$$

The current through series voltage source converter (VSC) and grid current is same. The supply current during sag condition is 46 A at 0.3p u, hence the VA rating of injection transformer obtained is 10 kVA

e) INTERFACING INDUCTOR OF SERIES FILTER CONTROLLER:

The rating is chosen based upon ripple current during swell condition, switching frequency and DC link voltage. Its value is expressed as,

f_{se}= switching frequency,

I_r = inductor current ripple, which is 20% of grid current.

$$L_r = \frac{\sqrt{3} \times mV_{dc}K_{SE}}{12af_{se}I_r} \quad (6)$$

Here, m=1, a=1.5, f_{se}=10 kHz, V_{dc}=700 V and 20% ripple current, one gets 3.6mH as selected value.

2) CONTROL OF UPQC INTEGRATED SOLAR PV

Shunt filter controller corrects difficulties with load power quality, such as load current harmonics and reactive power. The series filter controller protects the load against grid side power quality problems such as sags and swells. PV integrated UPQC also serves as a power source for the solar PV array.

(i) SHUNT FILTER CONTROLLER:

By running the solar PV array at its maximum power point, the shunt filter controller pulls the maximum power from it. The reference voltage for solar PV DC-link UPQC's is generated by the maximum power point tracking (MPPT) method. The Perturb and Observe (P & O) technique and the incremental conductance algorithm are two extensively used MPPT algorithms [21]. (INC). The (P & O) algorithm is employed to implement MPPT in this work. A PI-controller is used to keep the DC-link voltage at the generated reference. The shunt filter controller takes the active fundamental component of the load current to perform load current compensation.

The shunt filter controller is regulated by employing the SRF approach to derive the fundamental active component of load current. The phase and frequency information collected from the PLL are used to convert the load currents to d-q-0 domain. Figure 2 illustrates the shunt's control structure. The PCC voltage is the PLL input. The load current's d-component (I_{Ld}) is filtered to obtain the DC component (I_{Ldf}), which is the fundamental component in the abc frame of reference. A moving average filter (MAF) is used to recover the DC component without compromising the dynamic performance. The moving average filter's transfer function is as chooses to follow

$$MAF(s)=\frac{1--e^{-T_{\omega}s}}{T_{\omega}s} \quad (1)$$

The moving average filter's window length is Tw. Tw is kept at half of the fundamental time period because the lowest harmonic present in the d-axis current is a double harmonic component. The MAF has a DC gain of unity and a gain of zero for integer multiples of the window length. The PV array's corresponding current component is written as,

$$I_{pvg} = \frac{2}{3}\frac{P_{pv}}{V_s} \qquad (2)$$

where P_{pv} is the PV array power and Vs is the PCC voltage magnitude In the d-axis, the reference grid current is expressed in,

$$I^*_{sd} = I_{Ldf} + I_{loss} - I_{pvg} \qquad (3)$$

Currents in the abc domain are transformed from I*sd. The gating pulses for the shunt converter are generated by comparing the reference grid currents to the detected grid currents in a hysteresis current controller.

(ii) SERIES FILTER CONTROLLER:

The series filter controller injects voltage in the same phase as the grid voltage. This means it can be used to reduce the amount of voltage injected into the grid by a factor. The system is designed to provide energy optimum compensation for the power supply. References [20], [21] provide a comprehensive discussion of the various compensation mechanisms utilized for series filter control. The internal structure of the series filter control is depicted in Figure 3.

A PLL is used to extract the fundamental component of PCC voltage. This is then used to generate the reference axis in the dq-0 domain. These signals are translated to the 'abc' domain and sent via a pulse width modulation (PWM) controller.

(3) FUZZY LOGIC IMPLEMENTATION

The PI controller in the internal structure of the shunt filter controller is replaced with a Fuzzy Logic Controller as it has the advantages of a broad range of operating conditions, models the nonlinear functions of arbitrary complexity, solves the problems with imprecise and incomplete data and so.

The first step in creating a fuzzy controller like this is to define the range of values for the controller's input and output variables. As shown in Fig.12. The 1st Input variable is 'E', 2nd input variable is 'CE' and the output_variable. Here 'E' is error $(V_{ref} - V_{pv})$and 'CE' is change in error (Δ_{error}).

The reference voltage and PV panel voltage are compared and the error and change in error are given as inputs to FLC. The FLC generates a reference signal for a duty cycle of PWM which is applied to the switch of the boost converter so that the PV panel is continuously operated at maximum operating point MPP. The fuzzy controller takes the input value, does the computations based on the rules and then outputs the result. The Fuzzy Inference Process is the name of this method. Using the three steps it works.

1) Fuzzification
2) Evaluation of the rules
3) Defuzzification

The rule base for implementing modified PI controller which is Fuzzy logic controller is shown in the form of a 7×7 $matrix$ below.
Where, NB= negative big, PS= positive small, NM=negative medium, PM=positive medium, NS=negative small, PB= positive big, ZE=zero error.

	NB	NM	NS	ZE	PE	PM	PB
NB	NB	NB	NB	NB	NM	ZE	PS
NM	NB	NB	NB	NM	NS	PS	PM
NS	NB	NB	NM	NS	ZE	PM	PB
ZE	NB	NM	NS	ZE	PS	PB	PB
PS	NM	NS	ZE	PS	PM	PB	PB
PM	NS	ZE	PS	PM	PB	PB	PB
PB	ZE	PS	PM	PB	NS	ZE	PB

FIGURES

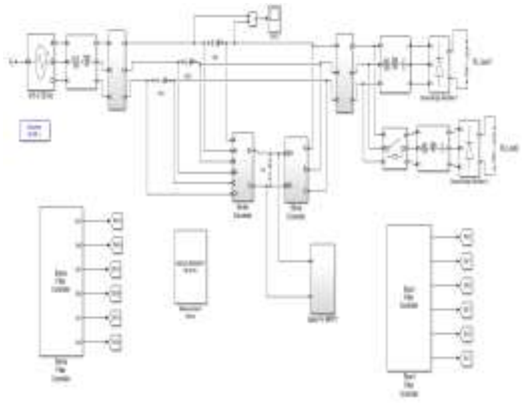

Fig.1 Simulation diagram of UPQC integrated Solar pv MPPT

Vol 12, Issue 7, July/2021
ISSN NO:0377-9254

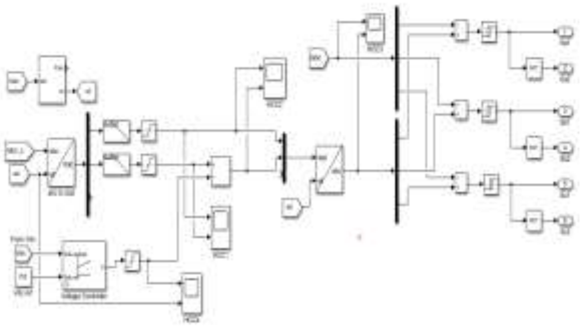

Fig.2 Internal structure of shunt filter controller

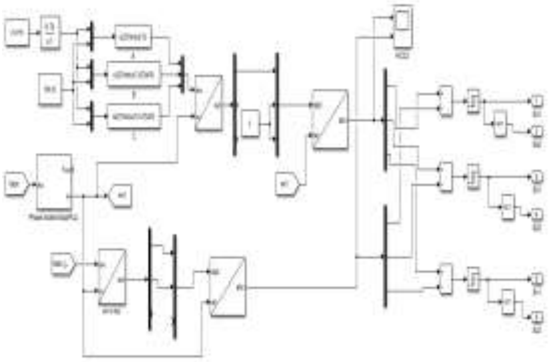

Fig.3 Internal structure of series filter controller

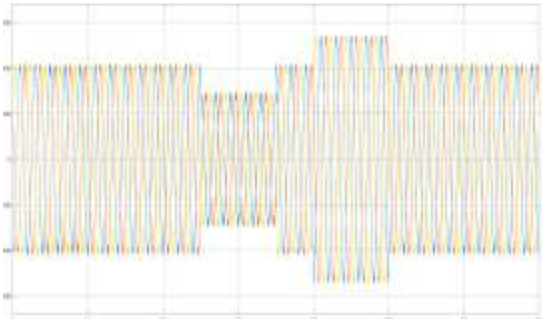

Fig.4 Waveform of source voltage with sag and swell(X-axis: time in sec, Y-axis: voltage in volts)

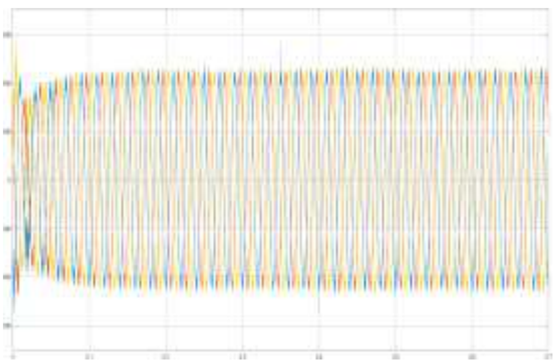

Fig.5 Waveform of load

voltage

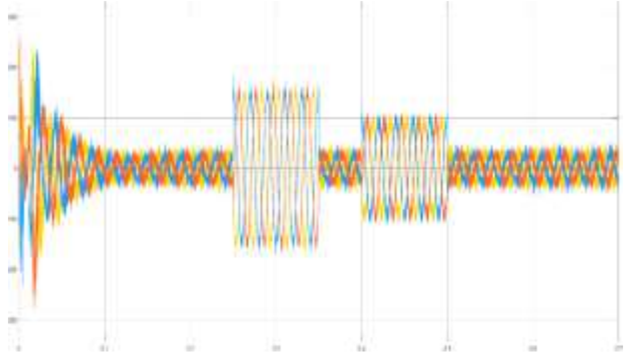

Fig.6 Waveform of Injected voltage

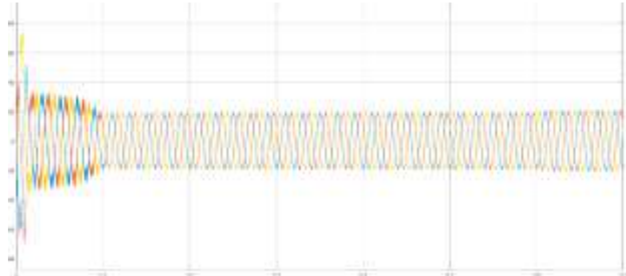

Fig.7 Waveform of source current

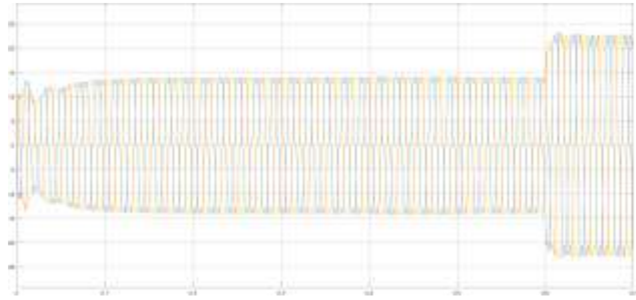

Fig.8 Waveform of load current

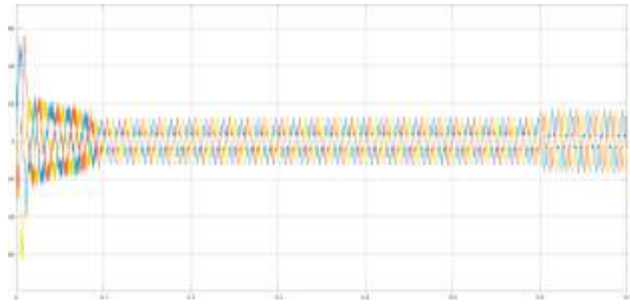

Fig.9 Waveform of Injected current

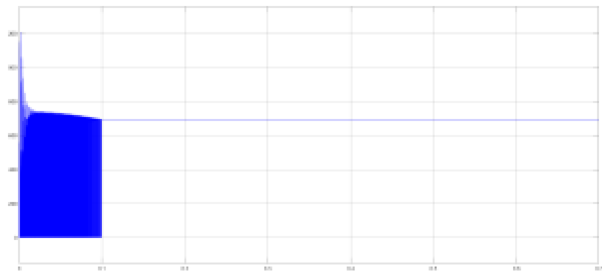

Fig.10 Waveform of voltage across Vdc

Vol 12, Issue 7, July/2021
ISSN NO:0377-9254

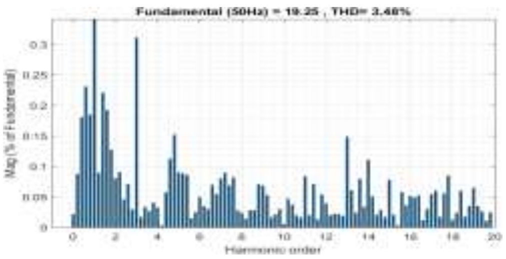

Fig.11 THD of source current is 3.48%

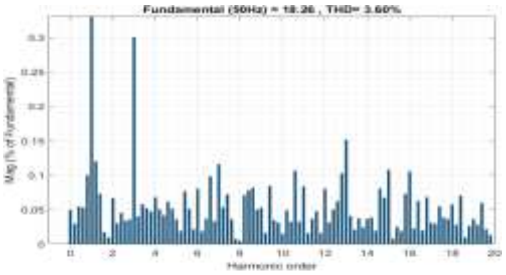

Fig.12 THD of source current without FLC is 3.60%

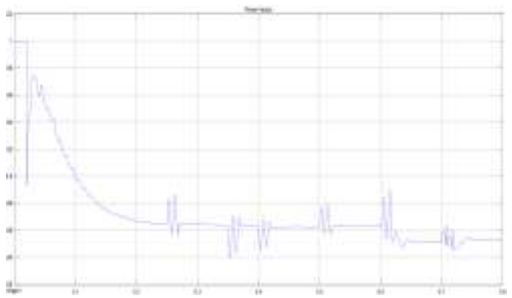

Fig.13 Power factor without UPQC integration is 0.8531

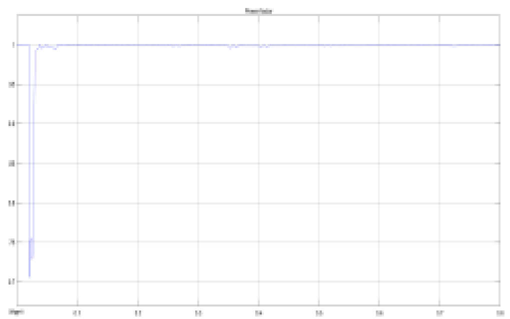

Fig.14 Power factor with UPQC and FLC integration is 0.999

CONCLUSION

The solar PV integration with UPQC reduces power quality issues such as voltage sag, voltage swell induced by non-linear loads and keeps grid current THD below acceptable ranges. Shunt filter controllers compensate for current issues by injecting current and regulating reactive power. The series filter controller compensates for voltage issues by injecting voltage and regulating active power.

By the above simulations, it is seen that the power quality improvement is achieved by integrating solar photo voltaic array with Unified power Quality Conditioner (UPQC) which can be seen from reduced total harmonic distortion (THD) of 0.12%. The Power factor has also been improved from 0.8531 to 0.999 (approximately unity power factor).

REFERENCES

[1] Y. Yang, P. Enjeti, F. Blaabjerg, and H. Wang, “Wide-scale adoption of photovoltaic energy: Grid code modifications are explored in the distribution grid,” *IEEE Ind. Appl. Mag.*, vol. 21, no. 5, pp. 21–31, September 2015

[2] M. J. E. Alam, K. M. Muttaqi, and D. Sutanto, “An approach for online assessment of rooftop solar pv impacts on low-voltage distribution networks,” *IEEE Transactions on Sustainable Energy*, vol. 5, no. 2, pp. 663–672, April 2014.

[3] J. Jayachandran and R. M. Sachithanandam, “Neural network-based control algorithm for DSTATCOM under nonideal source voltage and varying load conditions,” *Canadian Journal of Electrical and Computer Engineering*, vol. 38, no. 4, pp. 307–317, Fall 2015.

[4] A. Parchure, S. J. Tyler, M. A. Peskin, K. Rahimi, R. P. Broadwater, and M. Dilek, “Investigating pv generation induced voltage volatility for customers sharing a distribution service transformer,” *IEEE Trans. Ind. Appl.*, vol. 53, no. 1, pp. 71–79, January 2017.

[5] E. Yao, P. Samadi, V. W. S. Wong, and R. Schober, “Residential demand side management under high penetration of rooftop photovoltaic units,” *IEEE Transactions on Smart Grid*, vol. 7, no. 3, pp. 1597–1608, May 2016.

[6] B. Singh, A. Chandra and K. A. Haddad, *Power Quality: Problems and Mitigation Techniques*. London: Wiley, 2015.

[7] M. Bollen and I. Guo, *Signal Processing of Power Quality Disturbances*. Hoboken: Johm Wiley, 2006.

[8] P. Jayaprakash, B. Singh, D. Kothari, A. Chandra, and K. Al-Haddad, "Control of reduced-rating dynamic voltage restorer with a battery energy storage system," *IEEE Trans. Ind. Appl.*, vol. 50, no. 2, pp. 1295– 1303, March 2014.

[9] B. Singh, C. Jain, and S. Goel, "ILST control algorithm of singlestage dual purpose grid connected solar pv system," *IEEE Trans. Power Electron.*, vol. 29, no. 10, pp. 5347–5357, Oct 2014.

[10] R. K. Agarwal, I. Hussain, and B. Singh, "Three-phase single-stage grid tied solar pv ecs using PLL-less fast CTF control technique," *IET Power Electronics*, vol. 10, no. 2, pp. 178–188, 2017..

[11] A. M. Rauf and V. Khadkikar, "Integrated photovoltaic and dynamic voltage restorer system configuration," *IEEE Transactions on Sustainable Energy*, vol. 6, no. 2, pp. 400–410, April 2015.

[12] S. Devassy and B. Singh, "Design and performance analysis of threephase solar pv integrated upqc," in *2016 IEEE 6th International Conference on Power Systems (ICPS)*, March 2016, pp. 1–6.

[13] K. Palanisamy, D. Kothari, M. K. Mishra, S. Meikandashivam, and I. J. Raglend, "Effective utilization of unified power quality conditioner for interconnecting PV modules with grid using power angle control method," *International Journal of Electrical Power and Energy Systems*, vol. 48, pp. 131 – 138, 2013.

[14] S. Devassy and B. Singh, "Modified p-q theory based control of solar pv integrated upqc-s," *IEEE Trans. Ind. Appl.*, vol. PP, no. 99, pp. 1–1, 2017.

[15] B. Singh and J. Solanki, "A comparison of control algorithms for dstatcom," *IEEE Transactions on Industrial Electronics*, vol. 56, no. 7, pp. 2738–2745, July 2009.

[16] B. Singh, C. Jain, S. Goel, A. Chandra, and K. Al-Haddad, "A multifunctional grid-tied solar energy conversion system with anf-based control approach," *IEEE Transactions on Industry Applications*, vol. 52, no. 5, pp. 3663–3672, September 2016.

[17] S. Golestan, M. Ramezani, J. M. Guerrero, and M. Monfared, "dq-frame cascaded delayed signal cancellation-based pll: Analysis, design, and comparison with moving average filter-based pll," *IEEE Transactions on Power Electronics*, vol. 30, no. 3, pp. 1618–1632, March 2015.

[18] R. Pea-Alzola, D. Campos-Gaona, P. F. Ksiazek, and M. Ordonez, "Dclink control filtering options for torque ripple reduction in low-power wind turbines," *IEEE Trans. Power Electron.*, vol. 32, no. 6, pp. 4812– 4826, June 2017.

[19] B. Subudhi and R. Pradhan, "A comparative study on maximum power point tracking techniques for photovoltaic power systems," *IEEE Transactions on Sustainable Energy*, vol. 4, no. 1, pp. 89–98, January 2013.

[20] A. Sadigh and K. Smedley, "Review of voltage compensation methods in dynamic voltage restorer DVR," in *IEEE Power and Energy Society General Meeting*, July 2012, pp. 1–8.

[21] A. Rauf and V. Khadkikar, "An enhanced voltage sag compensation scheme for dynamic voltage restorer," *IEEE Trans. Ind. Electron.*, vol. 62, no. 5, pp. 2683–2692, May 2015.